THE EXACT BER PERFORMANCE OF 256-QAM WITH RF CARRIER PHASE NOISE

Robert L. Howald, Ph.D.
Director, Transmission Networks Systems Engineering
Motorola Broadband Communications Sector

Abstract

The impact of phase noise on digital communications systems has been an ongoing challenge for system designers as modulations have become more complex, error corrections schemes have become highly sophisticated, and the channels under consideration become more varied. The HFC channel as used by CATV providers is a unique one from the phase jitter perspective, for a couple of key reasons. First, CATV is one of very few commercial uses of very higher order QAM, such as 64-QAM and 256-QAM, primarily because of the inherently high SNR and linearity due to the needed to support video. As a corollary to this point, as one of the few implementers of QAM, CATV is perhaps the only common example of a system that does so at RF frequencies. Secondly, precisely because the CATV plant was made with analog video in mind, the traditional channel was not designed with QAM in mind, including the equipment made for RF frequency generation. The result is upconverters and downconverters adequate for one application, and being asked to support another. While there is much to be thankful with respect to how digital signaling provides advantages all the way around, there are some possible "gotchas," and some overall confusion with respect to the phase noise topic. This paper is meant to describe and clarify these issues.

RAISING THE BAR

The use of 256-QAM has become increasingly popular in systems deploying digital signals in the forward band. There are several reasons for this. Most importantly, the expansion of the symbol set provides a 33% increase in bandwidth efficiency over 64-QAM. Also significantly, the SNR in the forward path is capable of supporting this sophisticated modulation format. Finally, the modem technology has become robust enough to handle the complexity of tracking, equalizing, and detecting 256-QAM symbols. As the constellation size has expanded, the sensitivity of the signal to forward path impairments has increased over and above the 6 dB difference in thermal noise sensitivity that exists between 64-QAM and 256-QAM. One of the impairments that can be particular troublesome if not understood is RF carrier phase noise. This impairment is imposed when baseband digital data is modulated onto an RF carrier, and again during upconversion. On the receive side, it occurs again in the tuner in the settop box in the home, and in any subsequent stage that takes the tuner's IF output to baseband for processing by the receiver. Additional RF processing in between that involves frequency translation, such as block conversion, would also cause degradation.

There has been continual concern from the operator community about just how clean the RF carriers need to be to support upgrading digital services to 256-QAM.

Questions have arisen in some systems over whether problems encountered during its roll-out are related to phase noise issues. Phase noise has a mysterious aura about it that can cause confusion about what exactly it is, how it qualitatively impacts the transmission, and, most of all, how this translates to quantified performance degradation. For high levels of QAM in particular, the effects of phase noise have sometimes been crudely approximated, and sometimes been portrayed as intractable except via measurement. However, the impairment is in fact, completely analytically tractable, and degradation due to it can be precisely predicted. In this paper, we will present the approach to this analysis and develop the analytical solution. The results will be used to generate exact predictions in the form of 64-QAM and 256-QAM BER versus SNR versus phase noise curves. The analysis will be supported with plots and constellations to clarify the phase noise problem.

PHASE NOISE

Carrier Noise Spectrum

Digital modulations that encode information in carrier phase are naturally sensitive to impairments that disturb this phase. Carrier phase jitter, which occurs because of the inability in a practical implementation to generate ideal sinusoidal signals, is such a process. Figure 1 shows the nature of phase noise in the frequency domain, in this case using a Motorola C8U upconverter. An ideal sinusoid is represented by a line spectrum. In the figure, such an ideal sinusoid would be represented by a vertical line at 0 Hz on the x-axis, which is not defined for this logarithmic scale. Instead, carrier noise energy at frequencies away from the ideal line are displayed along the y-axis, with the offset frequency from zero on the x-axis. While just one "side" of the carrier noise spectrum is displayed, a phase noise sideband at the same offset on the other side of the carrier has the same magnitude, and is anti-phase. There is a lower practical limit of offset frequency of interest in digital communications, because very slow phase noise as represented by very slow frequency variations are tracked at the receiver. In fact, as the zero frequency point is approached even more closely, the concept of phase noise is transformed into the concept of frequency stability, which characterizes the very slow frequency drift from the nominal center frequency associated with component and temperature variations of the circuitry. The amount that such carrier jitter disturbs detection is related to the QAM constellation's sensitivity to phase jitter, and the amount of this jitter that is imposed on the signal exists at the symbol detector.

As described above, there are two main components to the phase noise problem. Introduction of phase noise occurs during RF conversion. This includes both upconversion and downconversion. Figure 2 shows phase noise performance of a settop tuner, in this case tuned to 855 MHz. Note that the tuner's performance, as a low-cost, size-constrained, design, is significantly worse then the upconverter (Headend) piece. It is common for tuner performance to dominate the contributed RF phase noise. The phase noise spectrum at the tuner output represents essentially what is presented to the detection mechanism. The remaining IF conversion after tuning has minimal impact because of the effect of the upconverter and tuner, and because the downconversion from 44 MHz is a low frequency process, and thus less phase noisy.

The RF mixing that represents the points at which phase noise is introduced is one part of the two issues mentioned. The other part of this issue is the ability of the receiver to track the carrier phase. The amount of phase noise that is tracked is a spectral

function associated with the PLL filter processes involved in phase-locked carrier tracking. Basically, a PLL tracking loop follows the input reference noise roughly over its tracking loop bandwidth. Thus, it is incumbent upon receiver designers to understand the spectral mask of phase noise on the incoming signal, as well as the SNR characteristics of the received signal. A very wide bandwidth has advantages in its ability to acquire and track carrier phase relative to a narrowband tracking loop. The narrowband loop is less susceptible to false locking on spurious signals, and introduces less AWGN to the total phase error. The steady state tracking design is a trade-off of thermal noise degradation and phase noise degradation.

Quantifying Imposed Phase Noise

The quantification of the phase noise spectrum is determined by analyzing the frequency synthesizer design, which, in typical low cost commercial deployments, emphasizes low cost, direct divide PLL techniques. The performance of these PLL's can be modeled with computer aided mathematical analysis by understanding each of the noise sources and its contribution to the total noise performance.

Figure 3 represents an example of a simple synthesizer analysis that develops a phase noise prediction of a single-loop PLL synthesizer based on the relevant contributors to the output phase noise process. These include, primarily, the reference oscillator (crystal), the PLL logic devices, including phase detection and frequency division, and the voltage controlled oscillators (VCO's) that provide the RF output. Although this is a simple example, any level of synthesizer complexity it relatively easy to analyze, because PLL mathematics itself is quite straightforward.

On the receiver side, induced phase jitter is modified by the tracking mechanism. The receiver would include a tracking PLL, which could be analog or digitally implemented, depending at what level of receive downconversion is done. For single carrier modulations, times-N carrier recovery may be used, which still implements a PLL. In more advanced digital modems, decision-directed carrier recovery techniques may be used. The common Costas loop is a simple example. Regardless of mechanism, an untracked phase jitter component will exist at detection.

In Figure 4, the modification of carrier spectra and the resulting output error spectrum are shown. The output error spectrum in this case refers only to the difference between what phase noise spectrum is on the input, and what is on the output. While ideal phase noise would be to have none, an equally attractive case for performance would be one in which the receiver phase noise that is created by carrier tracking looks like that on the carrier, and thus the transmit and receive carrier references "move together," nullifying error. When they are not together, we have untracked phase noise, and this is the impairment mechanism under discussion.

It is important to note that in Figure 4, both phase noise and thermal noise elements are shown to bring out the trade-off. Incoming phase noise is tracked up to the loop lowpass bandwidth, creating a highpass spectrum for untracked jitter. However, the additive thermal noise contributes to the loop phase noise as a lowpass function, limiting the close to carrier noise spectrum by creating this thermal noise floor. This then represents the design trade-off – low-passed thermal noise versus high-passed phase noise.

EFFECTS ON QAM

The other key element in understanding the phase noise phenomenon is to recognize the sensitivity of the underlying modulation scheme to the jitter. The need for bandwidth efficiency, ease of implementation, and high performance, makes the QAM family of modulations an excellent choice in many applications. The constellation is an important visual tool in evaluating modem performance for QAM modulations. Each distortion has its own characteristic effect on the constellation pattern. Consider Figure 5. For AWGN only, as in this 64-QAM example, the pattern will display a Gaussian "cloud" around the ideal constellation point. By contrast, phase noise represents angular rotation of the symbol points, away from the ideal as shown in Figure 6. The phase offset has a disproportionate effect on the outer symbol points, because the length the received point moves away from the ideal point of the constellation is proportional to the radius associated with that symbol. Consider a square, four-sided decision region that is (2d x 2d) in area, with an ideal constellation point in its center at coordinates (x, y), and an error angle of ϕ due to phase noise like that shown in Figure 6. The shortest distance to each of the boundaries, without phase noise or any other impairment, is d in all directions. With the error ϕ, the four distances become modified, and shorter in two directions, to

$d1 = x \cos \phi - y \sin \phi - x + d$
$d2 = x + d - x \cos \phi + y \sin \phi$
$d3 = x \sin \phi + y \cos \phi - y + d$
$d4 = y + d - y \cos \phi - x \sin \phi.$

For M-QAM, the number of different symbol possibilities – the number of decision region squares – increases with M. Also, because of the relationship between the distance to a boundary and the symbol location on the constellation for a given phase noise error, ϕ, higher density QAM signals become highly sensitive to phase noise. Outer symbol points are increasingly far from the center of the constellation, and this distance multiplies the phase error, shortening the distance to the boundary. Simple schemes such as BPSK and QPSK are quite robust to phase jitter. The symbol boundaries for QPSK are a full 45 degrees away. As such, a large error in phase would have to occur for a symbol error to be made in detection due to just jitter. Such a value of phase jitter, measured most conveniently in degrees rms, is extremely unlikely to occur with any significance to effect most reasonable error rates. This is not the case for QAM modulations using many more symbol points, and phase noise specifications must carefully consider the effects on the outer symbols.

How a noisy phase carrier effects symbol error rate performance is relatively straightforward to determine for the BPSK and QPSK situations under the assumption that the phase noise process is "slow". In this case, relative to a symbol time, the carrier phase can be considered constant over a symbol time, although its phase varies in value among the symbols. Small angle assumptions ($\sin \phi \approx \phi$) are often used to simplify BER performance analysis. Also, the phase noise is often considered to be from AWGN in the tracking PLL's only. In the case of HFC, both of these tend to be poor assumptions, because the larger M is, the more significant knowing the angle of error precisely becomes. For example, whereas the QPSK example pointed out that the symbols were 45° degrees away from a boundary, this number for 64-QAM is reduced to 7.7°, and for 256-QAM to 3.7° on the outer symbol points. In addition, considering just AWGN as the cause of jitter in the tracking PLL may work well for low SNR links, such as satellite or wireless. However, for HFC, the link SNR is quite high (40 dB range), so the need to account

for the other phase noise variables is significant. Assuming that AWGN-only jitter contributions exist leads to the conclusion that no error rate floor will be seen. This is a treacherous conclusion for multi-level M-QAM when true carrier phase noise is included.

Summarizing, then, the ability to overlook or be minimally concerned with phase noise impairments in many operating links today is a function of the robustness of the classical BPSK and QPSK families of modulations, and the low SNR channels they were often associated with. There is potential for a substantially larger penalty as the constellation is expanded.

PHASE NOISE STATISTICAL ASSUMPTIONS

The phase noise process is assumed to take on Gaussian behavior, and for practical implementation and mathematical tractability reasons, will be assumed to be both ergodic and stationary. Each of these latter two are common assumptions when developing phase noise analysis in the context of its performance effects for systems applications. This assumption is typically made in analysis of the phase jitter process when the goal is something other than exact calculation of the statistics of phase noise. In analysis for communication systems, the assumption of Gaussianity is assumed roughly equivalently as often as using the assumption that the PDF is Tikhonov. The Gaussian assumption is, in fact, a more general assumption than Tikhonov. The latter is derived from the assumption of a sine wave plus AWGN input only to the PLL (i.e. no phase noise). As mentioned, for a CATV situation and its high SNR, this is not a good assumption. In the limit of high SNR, the Tikhonov PDF asymptotically approaches a Gaussian PDF. Additionally, the Tikhonov PDF is arrived at by assuming a first order PLL. The basic PLL structure here, and the dominant one in practice is the second order PLL topology.

The assumption of a Gaussian PDF leaves only the need to specify the two parameters that uniquely specify this distribution, the mean and the variance. A zero mean assumption (no steady state phase offset) leaves only the determination of variance, which represents phase jitter power. This can be determined by evaluating the phase noise spectrum over the region of interest that applies at symbol detection. This can be determined to some extent by phase noise measurements, although this type of equipment cannot easily decompose the spectrum into untracked and tracked phase jitter at a receiver. For design purposes, an accurate model is necessary. Such a model can be mathematically and empirically created by implementing the various PLL transfer and error functions, and applying expressions developed for the phase noise spectra of each of the various noise contributors into these models. Such an example was shown in Figures 3 and 4.

Untracked Phase Error

The spectrum of interest for systems analysis is that corresponding to untracked phase jitter, which is evaluated using the error function of the phase tracking process, the result of which is shown in Figure 4. Figure 4 has a highpass filter effect on the input phase noise mask. This highpass filter is the dashed frequency responses in Figure 4 at the top of the plot, and operates on an input spectrum such as Figure 2. Figure 4 looks similar to Figure 2 in the examples shown only coincidentally. The Figure 4 analysis assumed a thermal noise floor that creates the lowpass response, and the Figure 2 lowpass structure derives from high phase noise attributed to logic noise in the tuner design being amplified by the PLL. The tracking loop in the receiver will actually attenuate this region at 40 dB/decade if we

had visibility into that process, and the thermal noise added to the channel would instead result in a lowpass "floor" to replace it.

The spectrum derived from the model is used to calculate rms phase jitter by integrating the untracked jitter spectrum. The relationship between degrees rms and the composite integrated single sideband (SSB) phase noise in dBc (a negative dB value) is

$$\text{deg rms} = (180/\pi)\ \text{sqrt}\ [10^{\phi\ (\text{dBc})}]\ .$$

The approach here, then, is to use the phase noise spectra developed above through mathematical and numerical modeling. The key parameters are the untracked rms jitter imposed at detaction, and the bandwidth of interest over which it is imposed. The latter is a function of the signal bandwidth of interest at detection, which is basically tied to symbol rate.

BER EXPRESSION DEVELOPMENT

The BPSK and QPSK results have been derived in several classical reference papers. For constellations of higher order, less work has been done. However, these principles can be extended to larger constellations. For clarity, while this paper specifically addresses 256-QAM, the analysis will be explained using a much less cumbersome example, 16-QAM.

BER of 16-QAM with Phase Noise

The straightforward nature of QPSK analysis is due to the fact that each symbol is affected identically. Approaches to calculating degradation for larger constellations typically involved the small angle assumptions for sine and cosine. In this methodology, only the quadrature term contributes degradation and its variance can be added to the thermal Gaussian effects, since they are uncorrelated. The end result is a composite SNR, calculated as

$$(1/\text{SNR}_T) = (1/\text{SNR}_{\text{awgn}}) + (1/\text{SNR}_\phi).$$

This approach is troublesome when signal amplitudes vary in M-QAM. The SNR approach breaks down because it does not properly account for the effect of angular rotation on the outer decision boundaries. It considers all symbols equally impacted by the jitter, effectively ignoring the sensitivity of the outer symbols, which limit the performance. For QPSK, all symbols have the same magnitude. For M-QAM, the crosstalk created by phase noise is a Gaussian noise term. However, it is multiplied by a discrete stochastic term (the data symbol) that can vary in magnitude, creating a different composite random variable. Fortunately, their likelihood is known, and thus a symbol-by-symbol decomposition is possible. Removal of the small angle simplification is therefore tractable for the slow phase noise case, so a complete solution can be derived.

For 16-QAM, there are three "classes" of symbols to consider. As such, it is most convenient to proceed with the derivation from the standpoint of the constellation, shown in Figure 7. There are the inner four symbols that form a QPSK constellation within the 16-QAM symbol set, the four symbols on the outer corners, and the remaining eight symbols which are on the outer ring. For two symbols a distance "d" apart (same d as previously used), the probability of selecting the wrong symbol when immersed in AWGN which is Gaussian of variance σ^2 is $Q(d/2\sigma)$, when optimal detection is used. Here, Q(x) is the complementary error function

$$Q(x) = 1/\sqrt{2\pi}\ {}_x f^{\infty}\ \exp(-y^2/2)\ dy.$$

This result is a simple conclusion resulting from determining the probability of a sample of Gaussian noise of standard deviation, σ, from exceeding d/2. Symbols bounded on multiple sides produce coefficient multipliers that increase this to $2Q(d/2\sigma)$, $3Q(d/2\sigma)$, or $4Q(d/2\sigma)$ in the AWGN case. It can also be shown that the $(d/2\sigma)$ argument is equal to $\text{sqrt}(E_S/5N_O)$ for 16-QAM, which is also $\text{sqrt}(4E_b/5N_O)$ for 16-QAM. Also, $SNR = E_S/N_O$ in a Nyquist channel.

Consider the first inner symbol, (a,a), surrounded on all four sides, and dropping any $Q^2(x)$ terms that result from the analysis as negligibly small. For these inner symbols, attenuation and the crosstalk term are identical to that encountered in the QPSK situation, but the symbols in this case are bounded on both sides. Assuming the 16-QAM constellation shown previously, with constellation points at (±a, ±3a), then consider the inner symbol (a ,a). This gives

$$Pi(correct) = Pr[\ 0 < a\ (\cos\phi + \sin\phi) + n_i < 2a] = Pq(correct).$$

Here, Pi(correct) is the probability of correct detection in the "I" direction (the x-axis), and Pq(correct) is the probability of correct detection in the "Q" direction, and n_i is an AWGN noise sample. This can be written

$$Pi(correct) = Pr[\ -a\ (\cos\phi + \sin\phi)\ < n_i < 2a - a\ (\cos\phi + \sin\phi)].$$

Since the distance between points, d = 2a, this can be written

$$Pi(correct) = Pr[-d/2\ (\cos\phi + \sin\phi)\ < n_i < d/2\ (2 - (\cos\phi + \sin\phi))].$$

Based on the previously stated results regarding the complementary error function, this can be expressed
using Q(x) and recognizing the following properties of the function:

$$Pr\ (\ n_i > a\ ) = Q(a/2\sigma)$$
$$Pr\ (\ n_i < a\ ) = 1 - Q(a/2\sigma)$$

and

$$Q(-x) = 1 - Q(x).$$

The result for is

$$Pi(correct) = (1 - Q[(d/2\sigma)(\cos\phi + \sin\phi)])(1 - Q[(d/2\sigma)(2 - (\cos\phi + \sin\phi))]).$$

Define

$$Q1 = Q[(d/2\sigma)(\cos\phi + \sin\phi)]$$
$$Q2 = Q[(d/2\sigma)(2 - (\cos\phi + \sin\phi))].$$

Again, neglecting the $Q^2(x)$ terms, negligibly small for practical error rates,

$$Pi(correct) = [1 - Q1 - Q2].$$

Similarly,

$$Pq(correct) = [1 - Q1 - Q2].$$

Then, the probability of a correct symbol, Pr(correct), is

$$Pr(correct) = Pi(correct) \bullet Pq(correct) = [1 - 2\ Q1 - 2\ Q2].$$

The error probability is then simply

$$Pe(a,a) = 2\ Q1 + 2\ Q2\ ,$$

or

$$Pe(a,a) = 2\ Q[(d/2\sigma)(\cos\phi + \sin\phi)]\ + 2Q[(d/2\sigma)(2 - (\cos\phi + \sin\phi))].$$

This same error probability exists for the 16-QAM symbol (-a,-a). These two symbols make up an eighth of the total symbol set,

which means that the contribution of these symbols to the overall 16-QAM degradation can be written

$$Pe = \tfrac{1}{4}\, Q[\sqrt{(4E_b/5N_o)}(\cos\phi + \sin\phi)] + \tfrac{1}{4}\, Q[(4E_b/5N_o)(2 - (\cos\phi + \sin\phi))].$$

For the other two inner symbols (a,-a) and (-a,a), the only piece of the above analysis that changes is the sign in the crosstalk term. In the case here, that sign is reversed.

All of the symbols can be analyzed in this way, and various sets of symbols are impacted identically in terms of mathematical evaluation, with minor changes in signs and coefficients. It is also important to keep in mind that the result of averaging all of the symbol possibilities (each has 1/16 probability of being transmission) is a symbol error probability. A bit error probability is obtained by assuming the symbol error probability means the incorrectly selected symbol is a neighbor, and neighbors differ by one bit if properly (Gray) coded. This assumption is not a good one for all cases of symbol error, particularly those that are due to catastrophic events such as large interference or sync loss.

For a complete BER expression, then, this conditional probability is then averaged over the Gaussian PDF of the untracked phase jitter and numerically evaluated.

RESULTS

Figure 8 shows the uncorrected BER results for 256-QAM with untracked phase noise varying from .5º rms to 1º rms. Clearly, the sensitivity of 256-QAM to this impairment is on display. A good rule to remember for rms jitter is that a signal-to-phase noise ratio of 35 dB represents 1º rms, and the degree rms term is a "voltage", meaning .5º rms is a 41 dB signal-to-phase noise ratio. Clearly, with this 41 dB ratio, there is trouble at hand. At a BER of 1E-8, there is a 2 dB degradation, which is generally unacceptable. Just as clearly, more than .5º rms quickly becomes intolerable.

Figure 9 shows the performance for values leading up to .5º rms. It is apparent from this plot that the BER curve is beginning to "take off" and flatten out at .5º rms, when compared to .35º rms, which shows a degradation less than one dB. An untracked phase jitter specification in the .25-.35º rms shows a tolerable situation.

Figures 10 and 11 graphically display why 256-QAM becomes so touchy to increased phase jitter. The effect of the additional jitter is magnified on the outer symbol points, creating a more troublesome scenario for the .5º rms case. The outer symbols for this case extend significantly closer to the boundaries than do the .25º rms case, making them more likely to have an AWGN sample push them over the decision boundary.

Figure 12 shows an example of measured case that represents about .5º rms of untracked jitter. Test and verification of phase noise effects is not an easy thing to do, because generating specific amounts of phase noise is not straightforward. While is it easy to create a noise local oscillator by adding noise to its control input, this is not the same mechanism by which phase noise is generated in real oscillators. Thus, the phase noise spectrum may look similar, but for different reasons. However, by statistically assuming Gaussian behavior, statistical differences are likely to be less pronounced then by focusing on deriving exact PDF's.

In this case, there was no noise injection for phase noise, just a cascade of RF sources as would be part of an HFC system – a Motorola C6U upconverter, and Temic tuner

in front of a Broadcomm test demodulator. The untracked jitter number is an estimate based on the imposed phase noise measured due to upconverter and downconverter (tuner) together, and knowledge and characterization of the test demodulator's tracking loop. Figure 2 shows a table of integrated phase noise values. This table breaks up the rms jitter contributions into spectral regions, and these regions combined with tracking bandwidth information lead to estimates of untracked jitter. As an example of the meaning of the rule of thumb previously given, the region between 1 kHz and 10 kHz from the carrier shows –31 dBc integrated noise power, or a signal-to-phase noise of 31 dB, which is about 1.6º rms.

With a 35 dB SNR in the 256-QAM channel (as measured by spectrum analyzer) the measured BER in the example of Figure 12 is about 3.7E-7, against theory that predicts about 9E-8. As a favorable sign, the realized BER measurement is slightly worse. In this case, the theory and measurement differ by about only .75 dB SNR. Note that the scale of Eb/No and SNR are the same, merely offset by 10 log 8 = 9 dB, because 256-QAM contains eight bits per symbol.

For comparison a 64-QAM example using the same RF setup is shown. Figure 13 shows the expectation of 64-QAM as a function of phase noise, and points out that .5º rms is an acceptable value in this case, whereas 1º rms begins to become problematic. This example runs error free, because of both the high SNR and the (relatively) low phase noise imposed. Figure 14 shows through the broad clear area around the constellation points why this is so.

Error Correction

Sophisticated forward error correction (FEC), as is used on the forward path for digital video and data, has the powerful ability to correct many forward path sins, and phase noise is among them. However, phase noise is a burst error mechanism because the phase error varies generally very slowly relative to the symbol rate. In other words, the jitter energy has frequency content much lower than the symbol rate. Thus, if the phase error drifts enough to cause a symbol error, it is likely that it will cause multiple symbol errors for a sequence of symbols. The amount likely is related to the jitter energy bandwidth relative to the symbol rate. Of course, it is not desirable to utilize the FEC capability to clean up phase noise issues, as this leaves less "margin" to handle other simultaneous impairments that the FEC was actually implemented to handle.

CONCLUSION

The use of 256-QAM places stringent phase noise requirements on any RF system. In the case of HFC, the issue is helped by the fact that the channel in question is very high SNR, leaving significant flexibility in the design of carrier tracking loops, such that imposed phase noise by converters can be removed at detection. The nature of the systems today is that the performance of converters and tuners can be as such to create bit errors, although not enough to cause catastrophic error problems that can be characteristic of higher order QAM in phase noisy channels. In general, FEC will correct for this, but at the expense of less FEC power available for other problems. More recently, lower phase noise equipment designs, made specifically to address high order QAM systems, have eased concerns about phase noise impairments. A complete analysis of a quality upconverter and a low phase noise tuner, coupled with a relatively wideband tracking receiver, can show that there adequate phase noise performance for 256-QAM transmission. The same analysis will also show that older equipment may yield acceptable, although impaired,

uncorrected BER results. However, the game once again changes if transmission standards evolve to 1024-QAM. A rough analysis shows that this modulation will be looking for better than .1º untracked rms jitter.

References

Howald, R., The Communications performance of Single-carrier and Multi-carrier Quadrature Amplitude Modulation In RF Carrier Phase Noise, UMI Dissertation Services, Ann Arbor, MI, 1998.

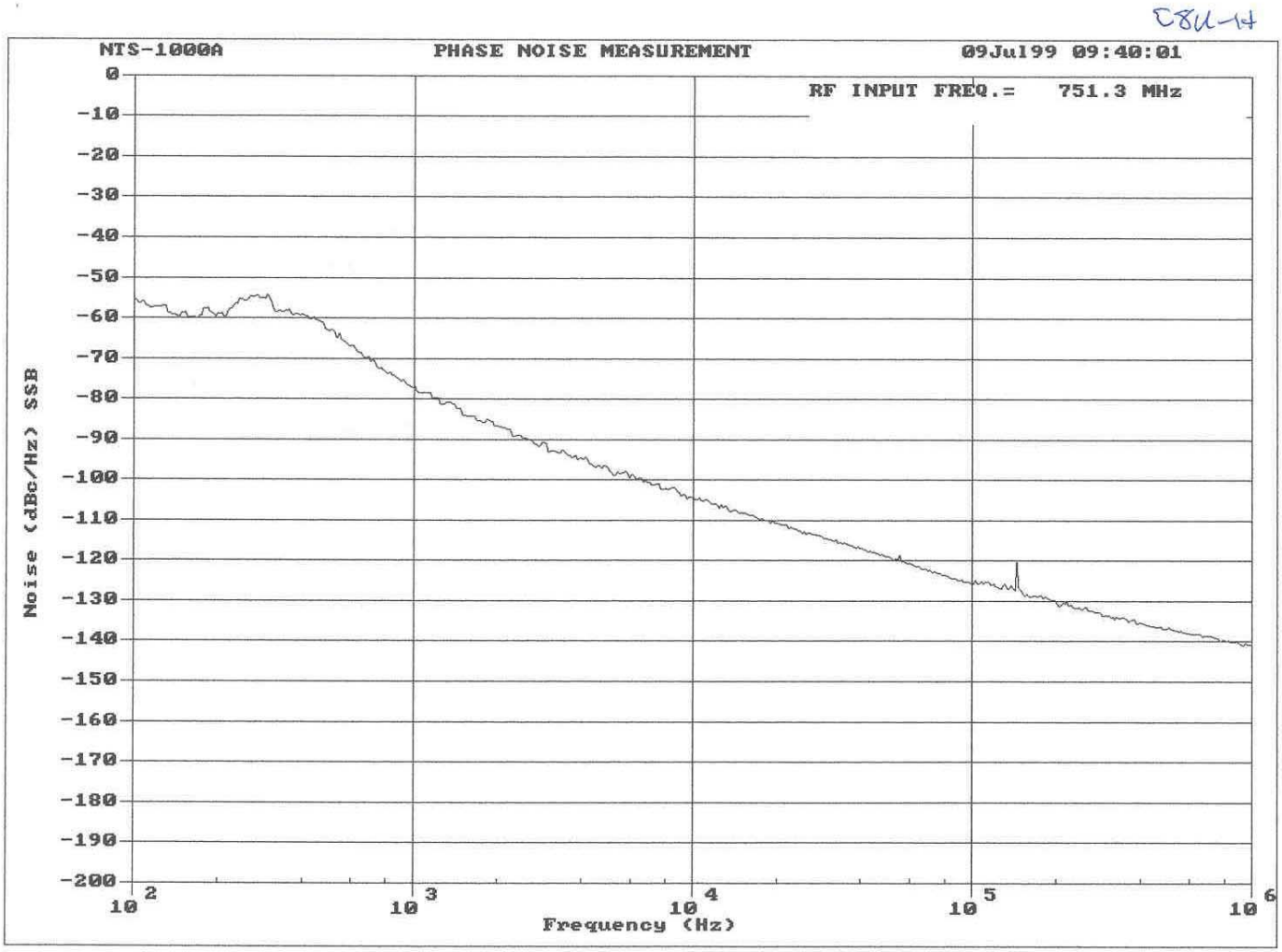

Figure 1 – RF Carrier Phase Noise Imposed by C8U at 750 MHz

17 MAR 99

BCM93180 Demod w/ 855.25 input

INTEGRATED NOISE LIST

START FREQ	STOP FREQ	INTEG NOISE	INTEG NOISE-SPURS
10.0 Hz	100.0 Hz	-10.0	-10.2
100.0 Hz	1000.0 Hz	-5.5	-8.5
1000.0 Hz	10000.0 Hz	-31.2	-31.4
10000.0 Hz	100000.0 Hz	-43.1	-43.3
100000.0 Hz	1000000.0 Hz	-48.0	-48.3

Figure 2 – RF Carrier Phase Noise Imposed by Tuner at 855 MHz

Closed Loop PLL Response, Inside Loop BW Noise, Oscillator Noise, and Total Phase Noise Response

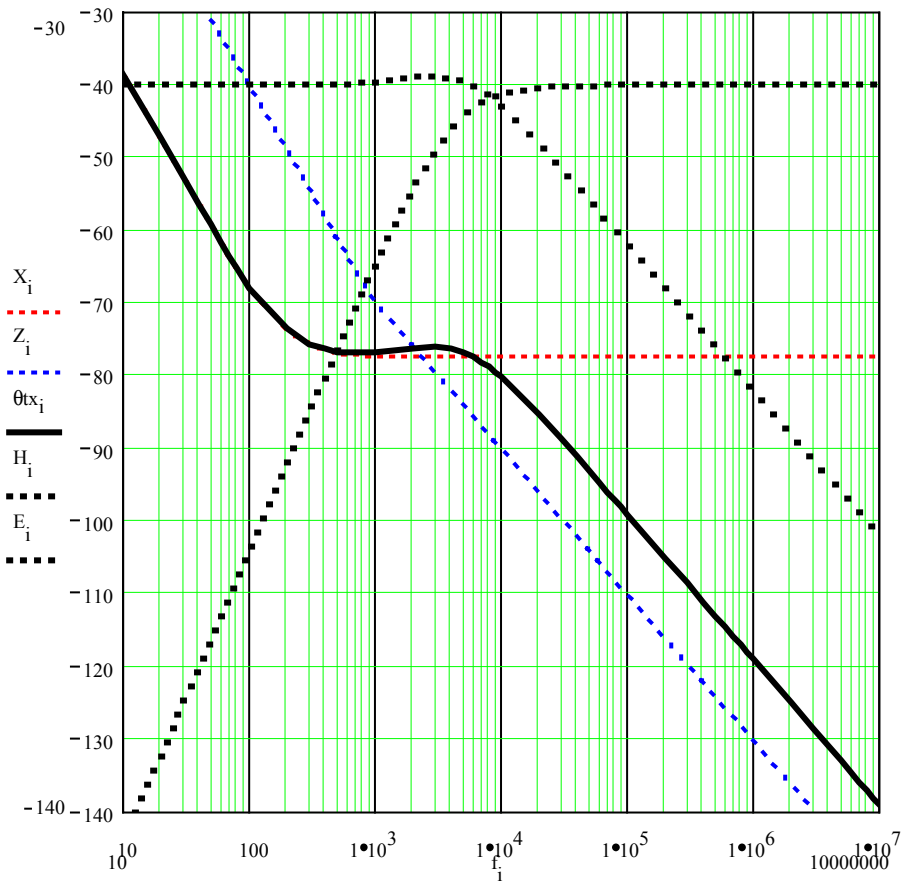

Figure 3 – Example Development of RF Carrier Phase Noise Spectrum from Synthesized Source

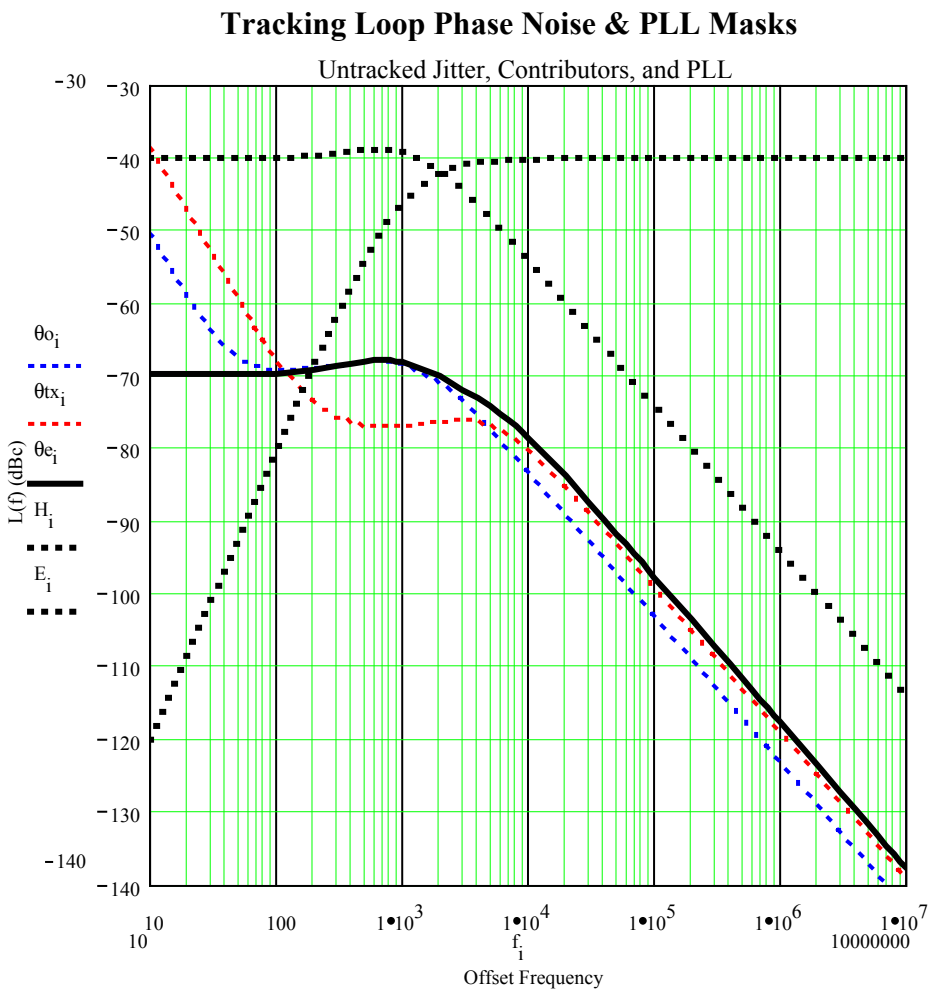

Figure 4 – Example Development of Demod Input Untracked Phase Noise Spectrum of AWGN & ϕ_n

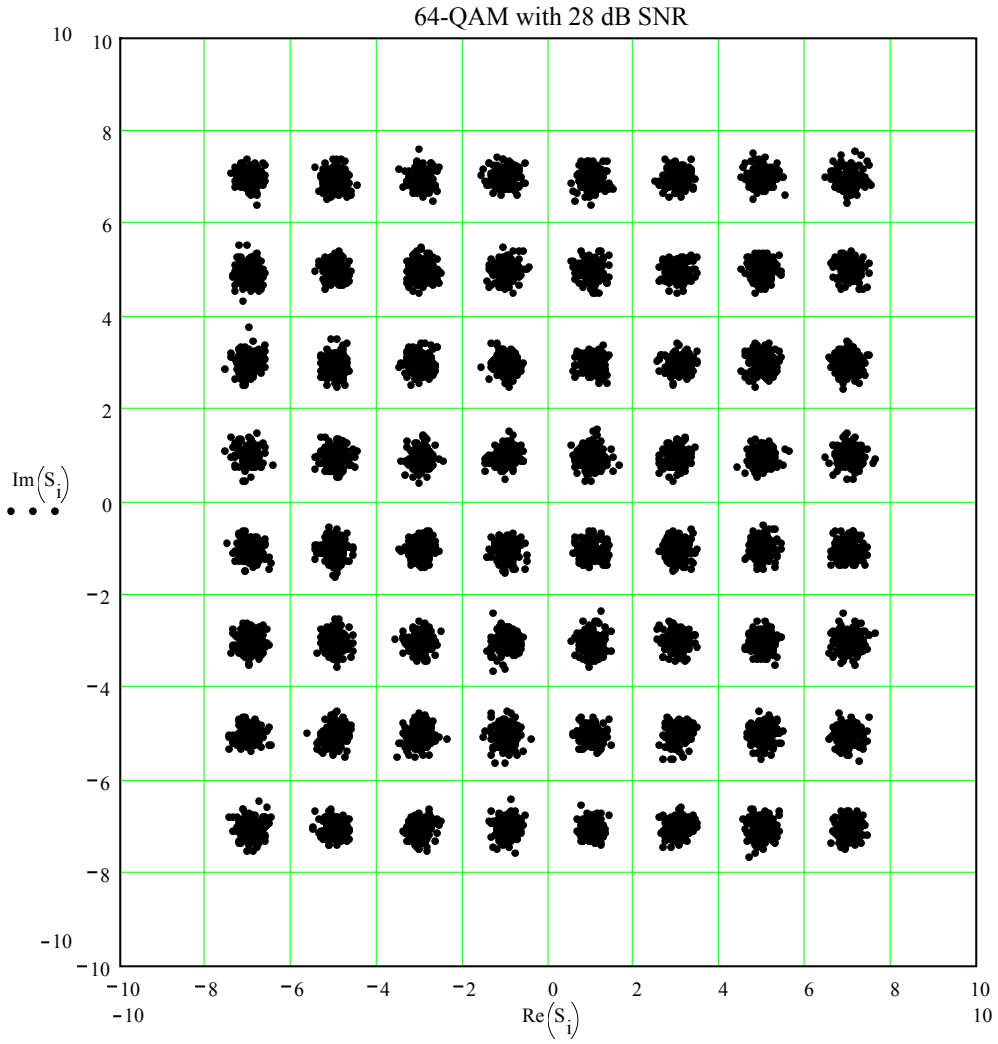

Figure 5 – 64-QAM with 28 dB SNR (BER ~ 1E-8)

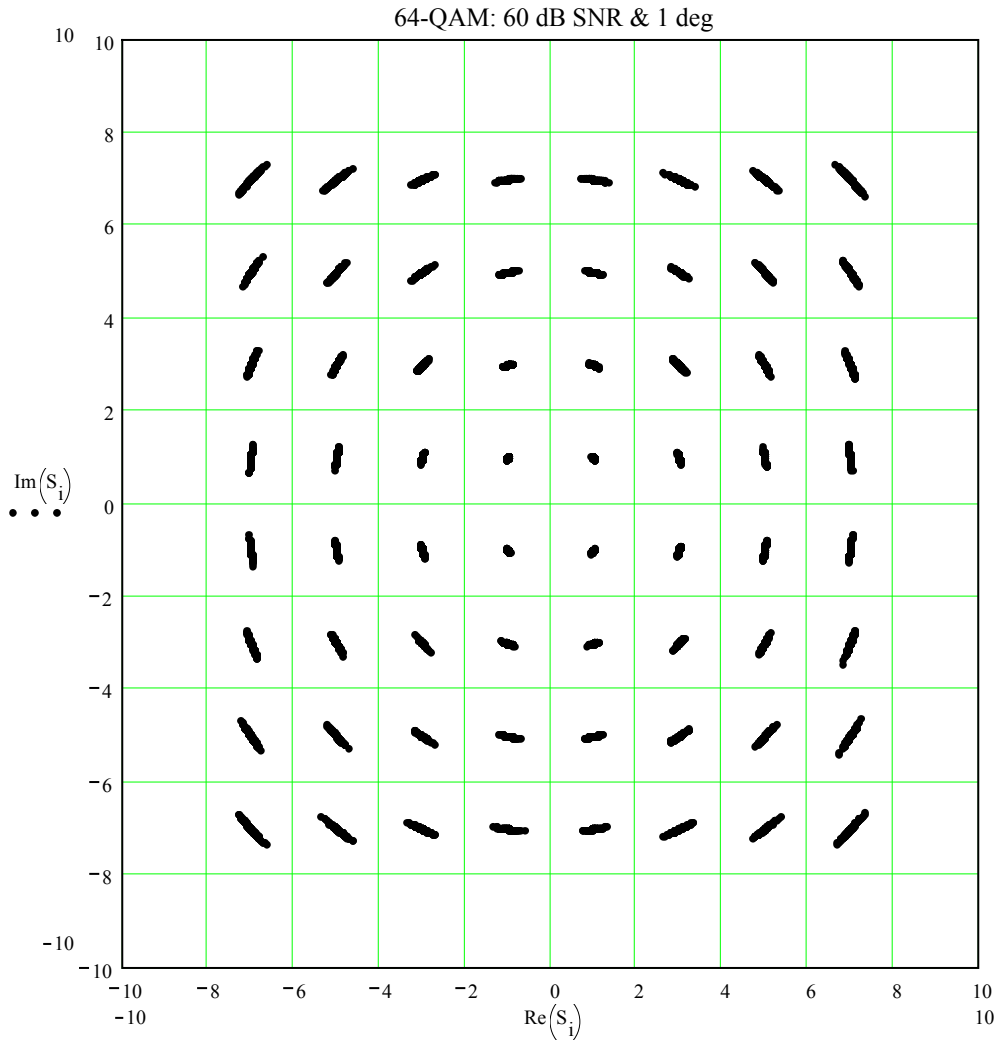

Figure 6 – 64-QAM with 60 dB SNR and 1 deg rms Phase Noise

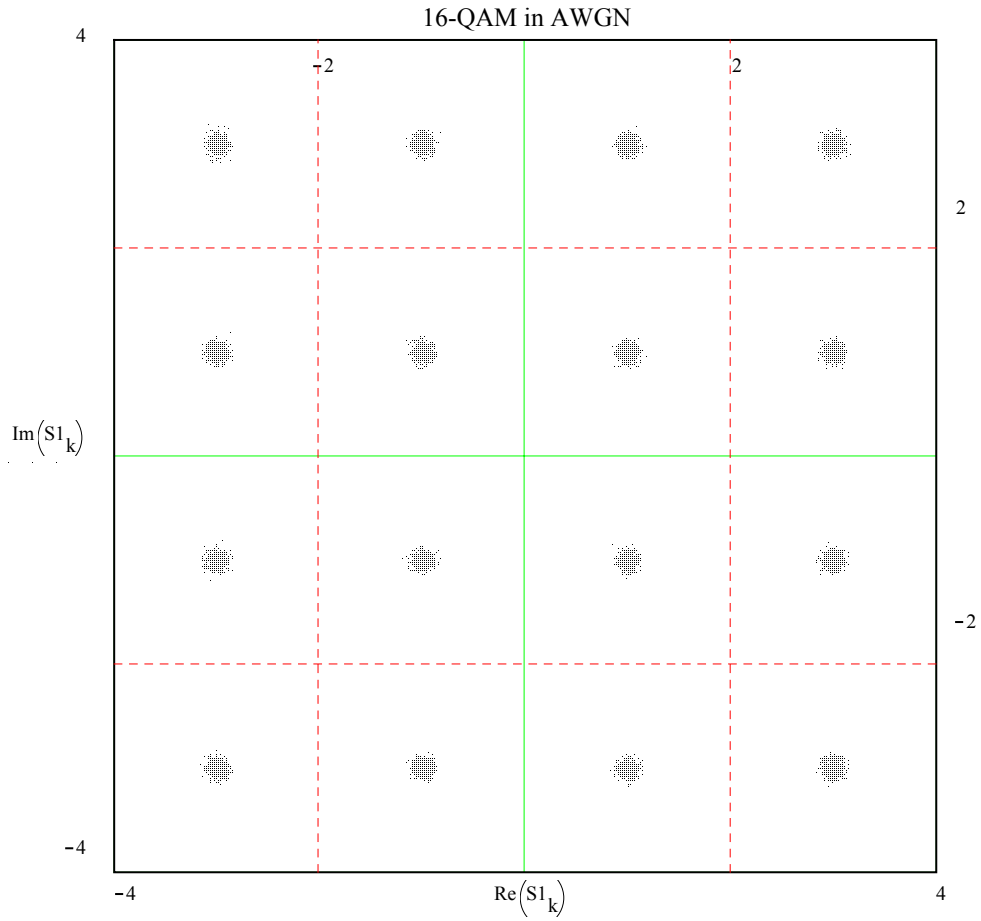

Figure 7 – 16-QAM in AWGN (SNR = 33 dB)

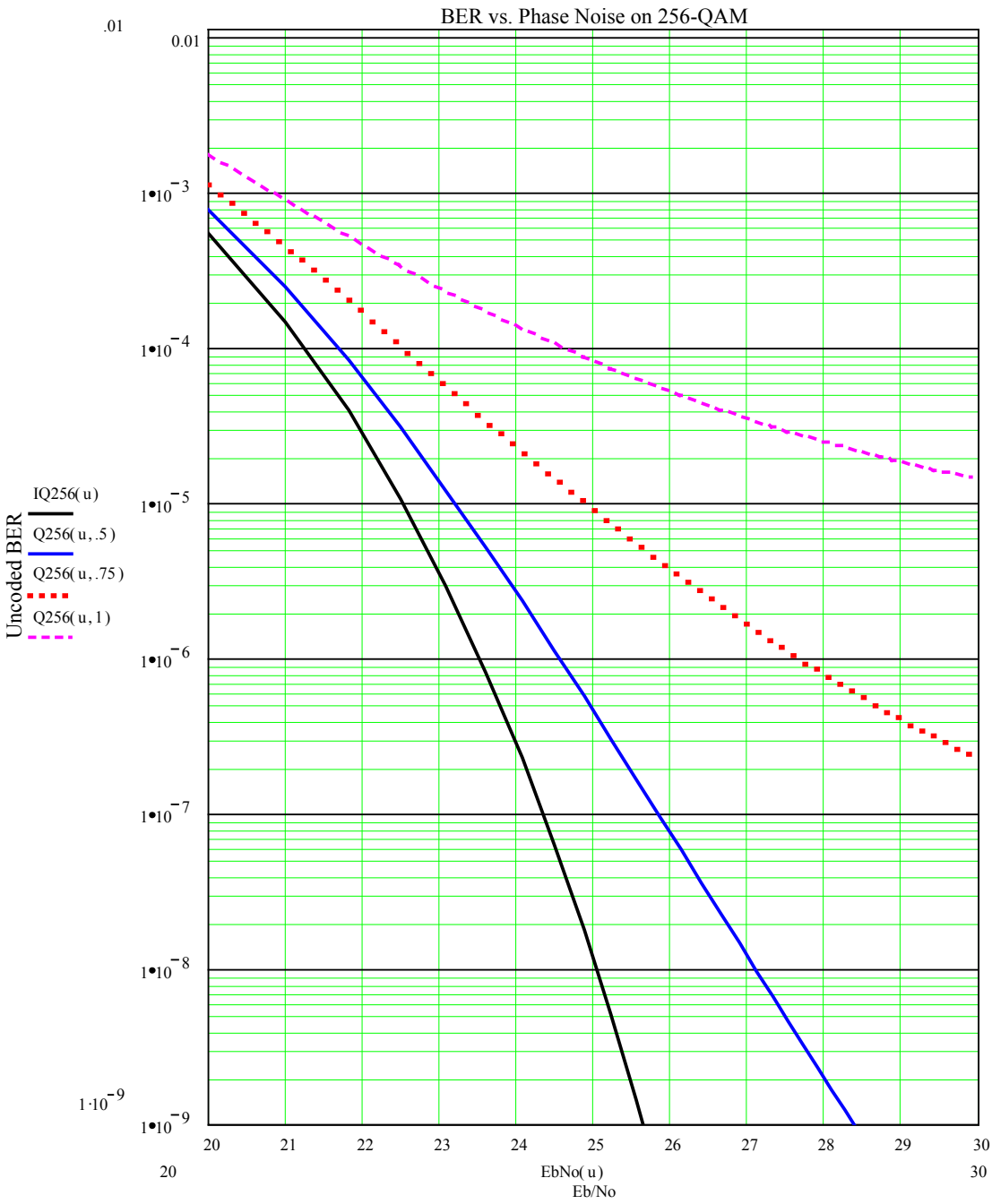

Figure 8 - 256-QAM BER with .5°, .75° and 1° rms of Gaussian Untracked Phase Jitter

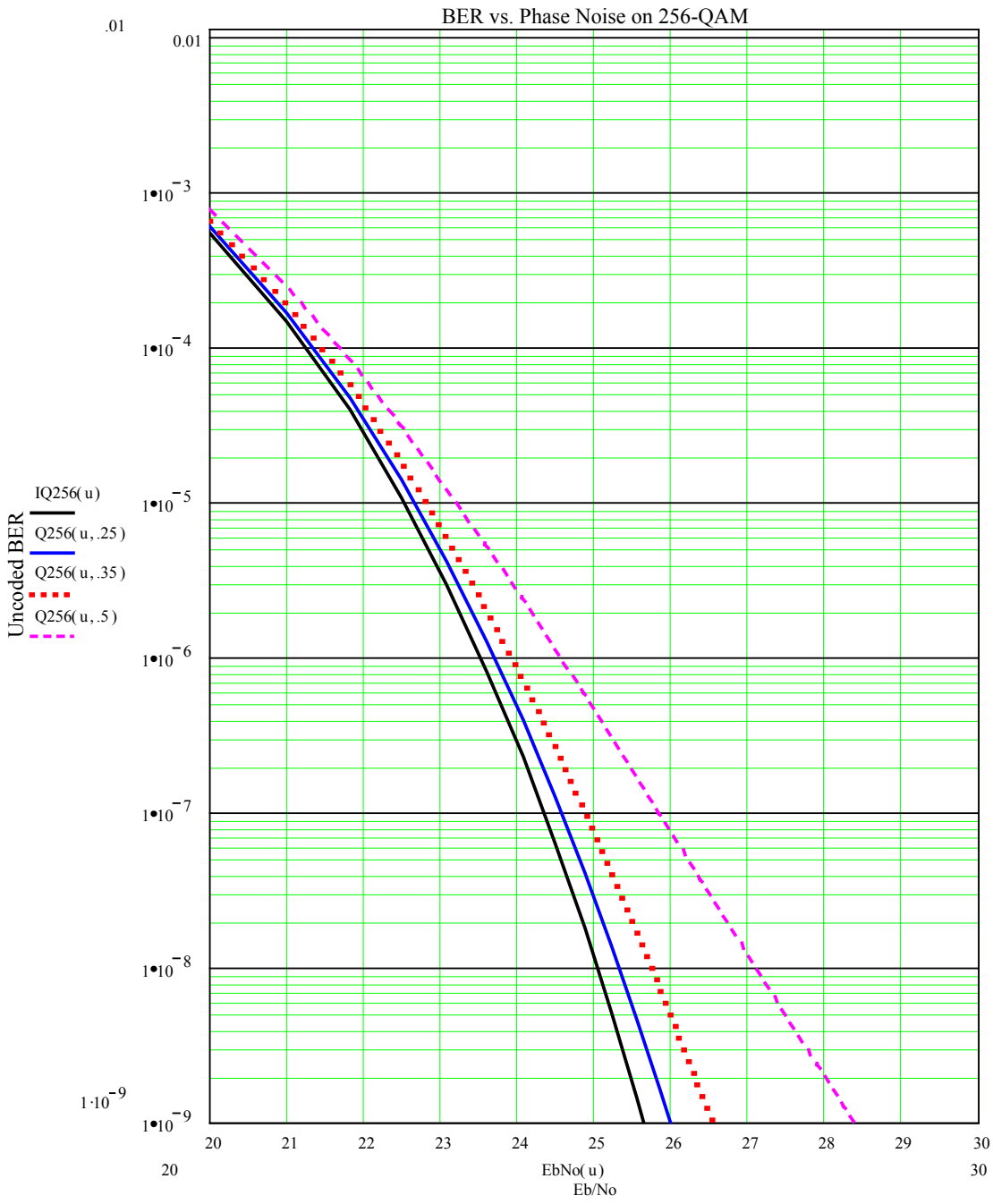

Figure 9 - 256-QAM BER with .25°, .35° and .5° rms of Gaussian Untracked Phase Jitter

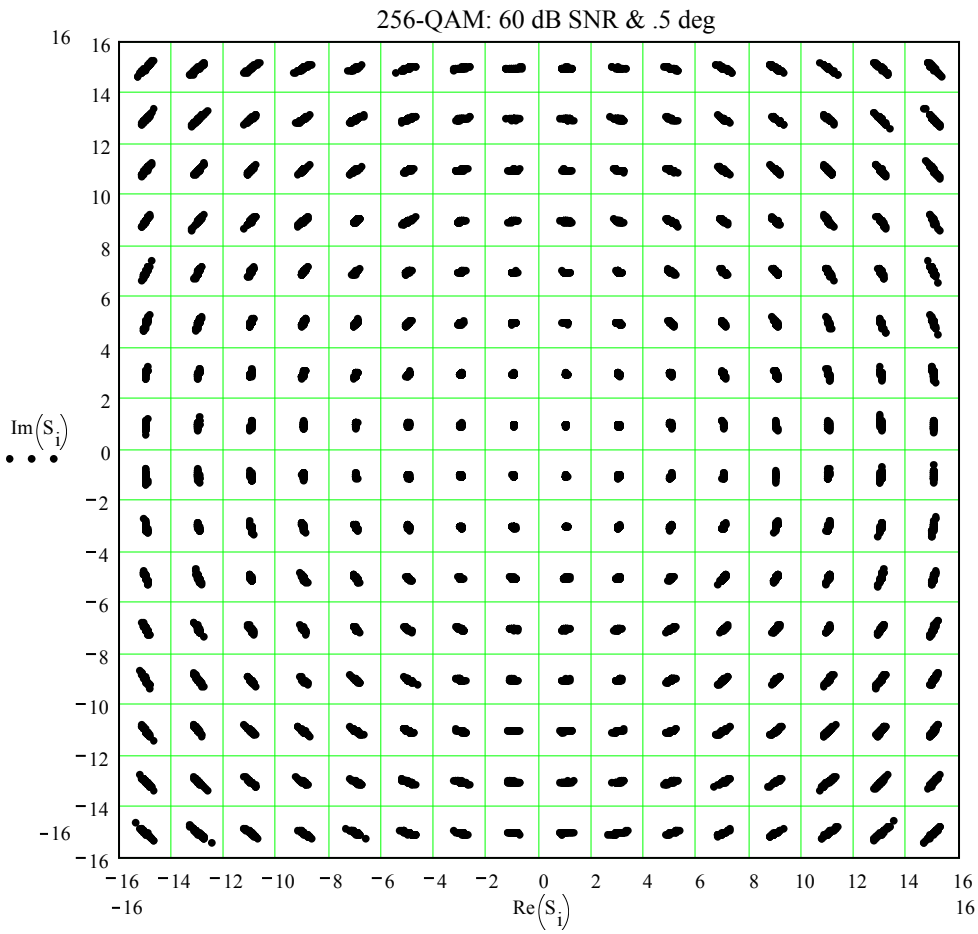

Figure 10 - 256-QAM Constellation with .5° rms Untracked Phase Jitter

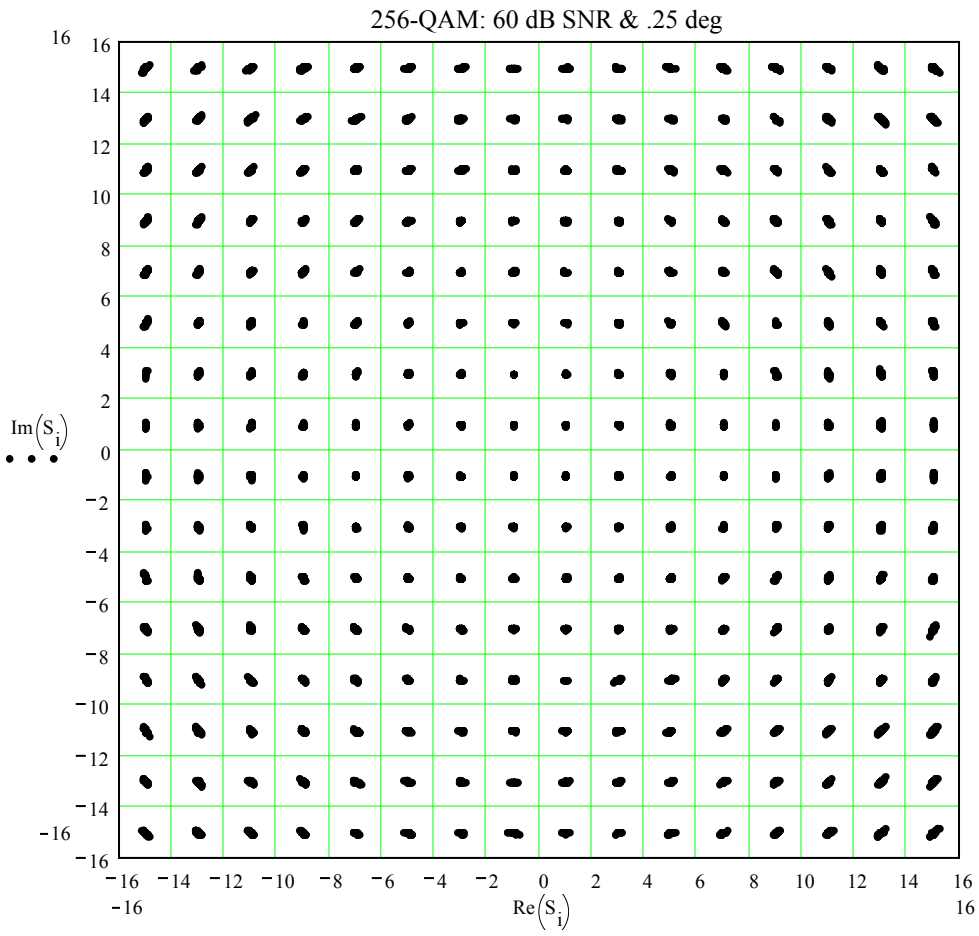

Figure 11 - 256-QAM Constellation with .25° rms Untracked Phase Jitter

256-QAM @ 35 dB SNR (Eb/No = 26 dB), 600 MHz (approx .5 deg rms)

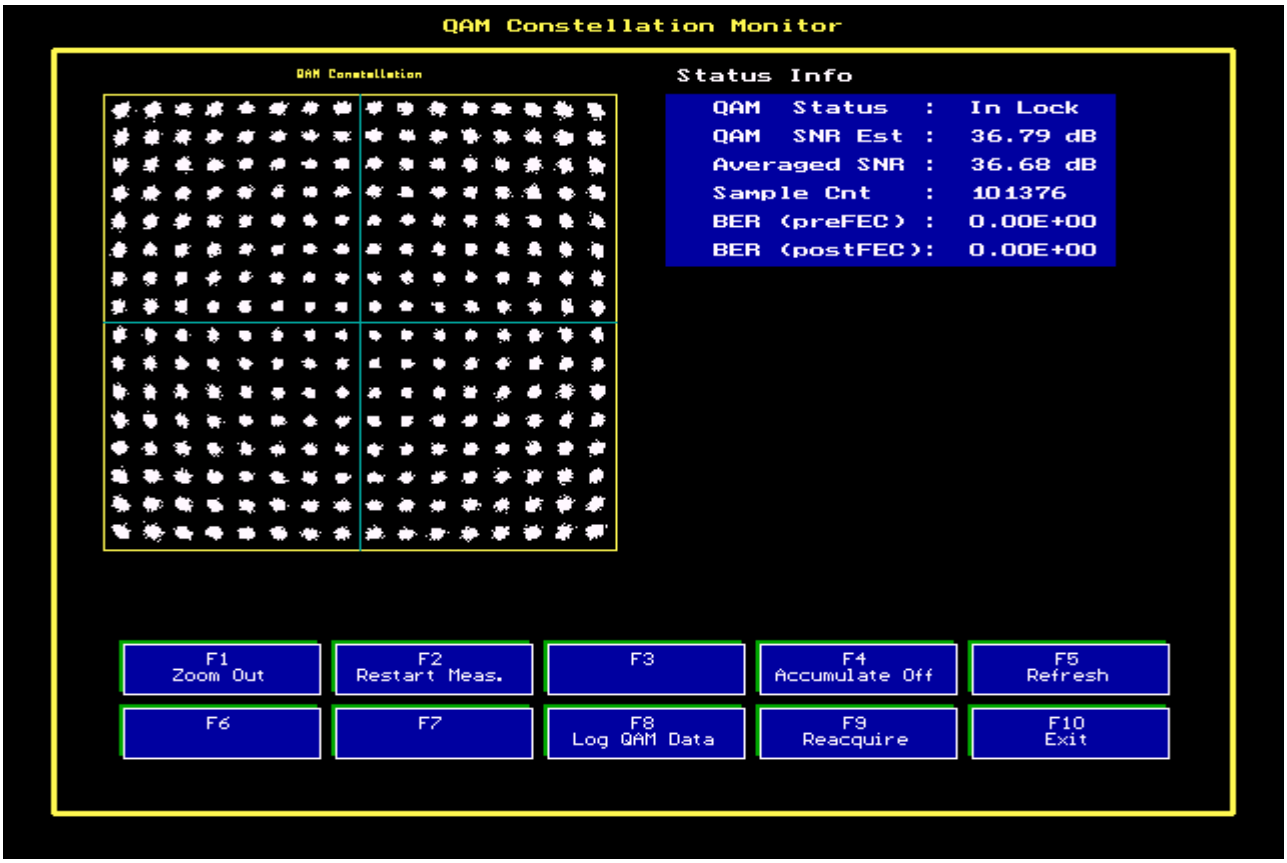

Predicted BER via Analysis = 9 E-8
Measured BER = 3.7 E-7
SNR Error Delta ~ .75 dB

Figure 12 – Measured 256-QAM (SNR = 35 dB) with .5° rms Untracked Phase Jitter

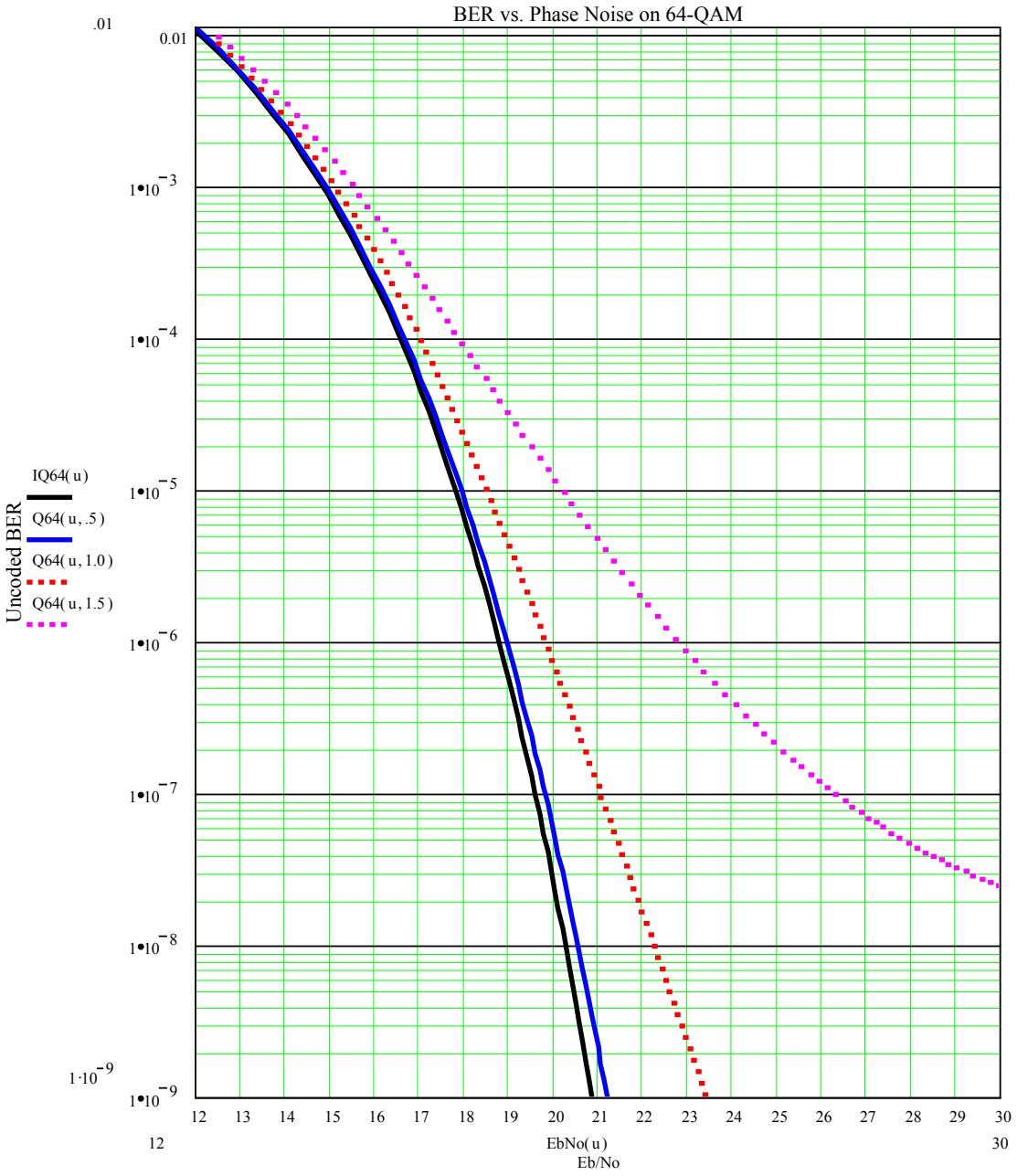

Figure 13 - 64-QAM BER with .5°, .1° and 1.5° rms of Gaussian Untracked Phase Jitter

64-QAM @ 35 dB SNR (Eb/No ≈ 27 dB), 600 MHz (approx .5 deg rms)

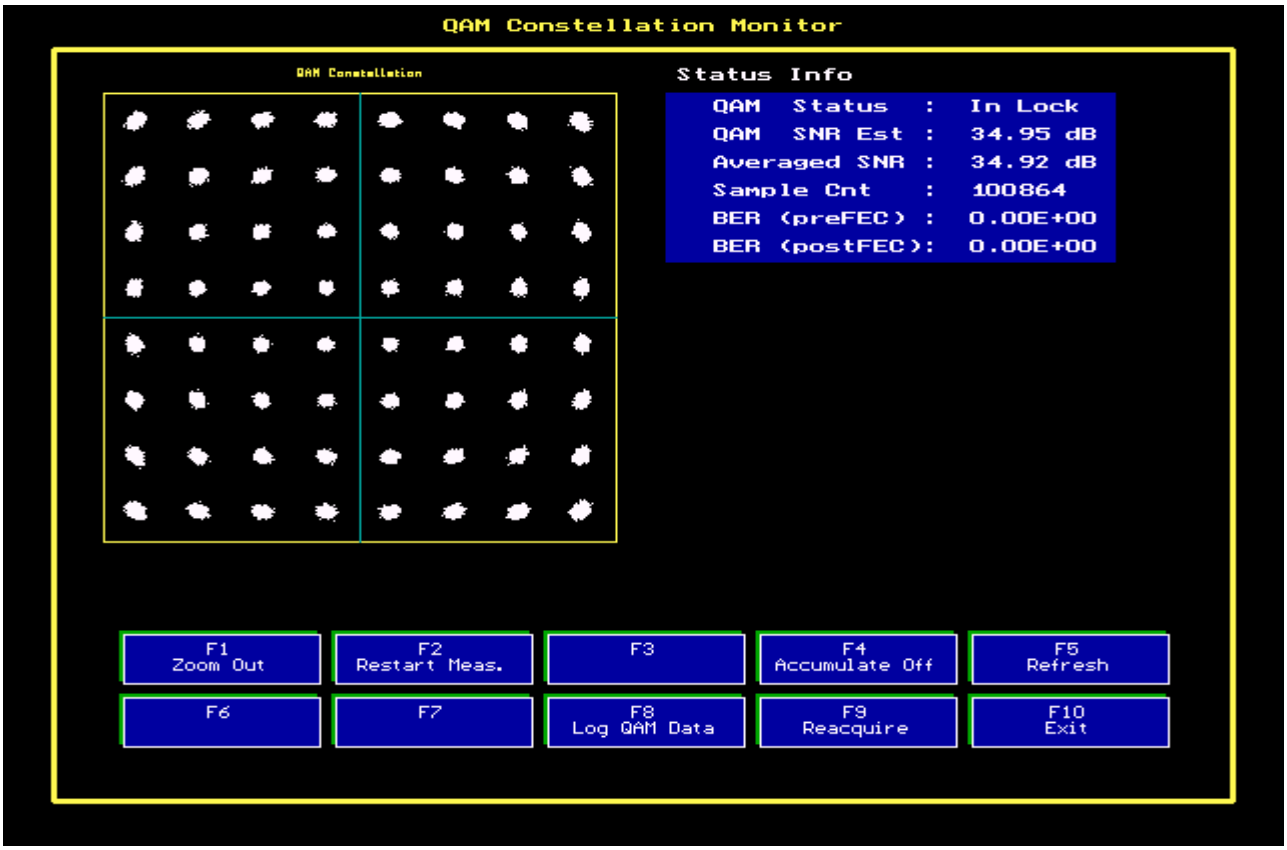

Figure 14 – Measured 64 -QAM (SNR = 35 dB) with .5° rms Untracked Phase Jitter